Airfoil optimization with CST-parameterization for (un-)conventional demands

Conference Paper · July 2018

CITATIONS
13

READS
2,621

3 authors:

Johannes Achleitner

16 PUBLICATIONS **77** CITATIONS

SEE PROFILE

Kai Rohde-Brandenburger

German Aerospace Center (DLR)

10 PUBLICATIONS **39** CITATIONS

SEE PROFILE

Mirko Hornung

Bauhaus Luftfahrt e.V.

244 PUBLICATIONS **1,827** CITATIONS

SEE PROFILE

Airfoil optimization with CST-parameterization for (un-)conventional demands

Johannes Achleitner[1], Kai Rohde-Brandenburger[2], Mirko Hornung[1]

[1] *Technical University of Munich, Institute of Aircraft Design, Germany,* johannes.achleitner@tum.de

[2]*DLR, Institute of Aerodynamics and Flow Technology, Braunschweig, Germany,* kai.rohde-brandenburger@dlr.de

Abstract: For the development of modern airplanes new and "better" airfoils are needed. The design of a new airfoil is mostly done for a number of fixed design points by the inverse method and optimized by manual iteration. When changing the preliminary design of the airplane, the airfoil design parameters are changing continuously in the design process. Therefore a tool chain was created, which allows the parametric optimization of the airfoil and the connection with a 2D panel method with fully coupled boundary layer calculation (XFOIL) with an optimizer. This paper will show an approach for airfoil optimization using an enhanced parameterization method of the airfoil coordinates. It explains the tool chain and the influence of the parameters used. The validation results for optimizing typical main wing airfoils with and without camber changing flap are shown. Based on that validation for conventional airfoils, more complex airfoils for unconventional geometries can be optimized. First results for a high lift system on a morphing wing system for a sailplane are shown and discussed.

***Keywords*:** airfoil design, airfoil optimization, CST shape parametrization, morphing, variable geometry, XFOIL.

Introduction

Numerical airfoil optimization has been widely employed in aerodynamic design of airfoils for aircraft and in the wind energy sector. For instance the airfoils for the Diana 3 [1] sailplane are designed with this method by Kubrynski. For the parametrization of the airfoil the "shape function / class function" methodology (CST) proposed by Kulfan and Bussoletti [2] has been used in the presented work. It has some advantages over other parametrization methods, e.g. infinite leading edge slope, i.e. the airfoil has a round edge radius and a finite trailing edge angle

Airfoil optimization methodology

The airfoil optimization methodology is shown in Figure 1. A set of design variables defines a start airfoil which is translated to airfoil coordinates by the parametrization tool. The airfoil coordinates are imported into a modified XFOIL [3]. The derivatives, i.e. drag coefficients at different lift coefficients are calculated. The objective function is a weighted sum of the drag coefficients with physically motivated weights. An optimization algorithm changes the design variables in order to obtain a better airfoil. For an airfoil with a variable leading edge geometry a subset of extra design variables is used for the parametrization of the nose droop. After convergence an optimized airfoil is obtained.

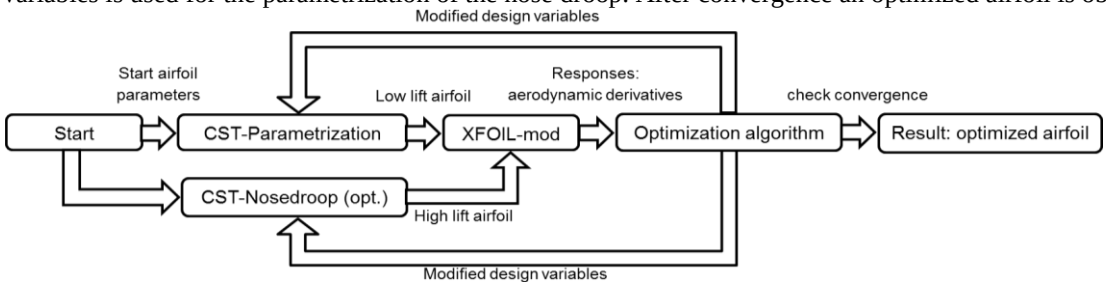

Figure 1. Airfoil optimization methodology

As optimization algorithm the Subplex algorithm is used, developed by Rowan [4]. It is a subspace line search method using a gradient free Nelder-Mead-Simplex [5] algorithm for optimization on the subdomains. A minimum thickness distribution for ensuring a minimum airfoil and flap thickness has been implemented. A minimum y/c coordinate at $x/c = 1.25\ \%$ was implemented to ensure that leading edge stall occurs beyond the normal angle of attack range with sufficient margin. Both constraints were added as penalty functions on the objective function. Some modifications have been made to the used XFOIL version, motivated by the observations of Timmer and van Rooij [6]. An improved post stall prediction is achieved by the adaptions proposed by van Rooij [7] and Hansen [8]. The drag prediction has been improved by implementation of the adaptions proposed by Ramanujam [9].

CST Parametrization of airfoils with and without camber changing flap

The contour line of the airfoil is expressed by two separate curves for top and bottom side, which are parametrized independently. The top and bottom contour lines, i.e. their z-coordinates as a function of its x-coordinates, are obtained by multiplication of a class function C(ψ) with a shape function S(ψ):

$$\zeta(\psi) = C(\psi)\, S(\psi) \qquad where: \qquad \psi = \frac{x}{c} \quad and \quad \zeta = \frac{z}{c} \tag{1}$$

The class function for the airfoil's top and bottom coordinates is defined as:

$$C(\psi) = \psi^{N_1}(\psi - 1)^{N_2} \qquad with \quad N_1 = 0.5 \quad and \quad N_2 = 1.0 \tag{2}$$

$N_1 = 0.5$ ensures a round leading edge with infinite slope at $\psi = 0$. For the trailing edge angle to be finite at $\psi = 1$, N_2 is set as $N_2 = 1.0$. Bernstein polynomials are used as weighted shape functions. The weighting factors x_i are the design variables for the optimization problem.

$$S(\psi) = \sum_{i=0}^{n} x_i\, B_i(\psi) \qquad where: \qquad B_i(\psi) = K_i\, \psi^i (1-\psi)^{n-i} \quad and \quad K_i = \binom{n}{i} = \frac{n!}{i!\,(n-i)!} \tag{3}$$

Figure 2 shows the CST parametrization of an airfoil with 5 CST parameters each on bottom and top side. The Bernstein polynomials are shown in the middle graphs. They are already weighted. The resulting shape function is shown as a colored line each.

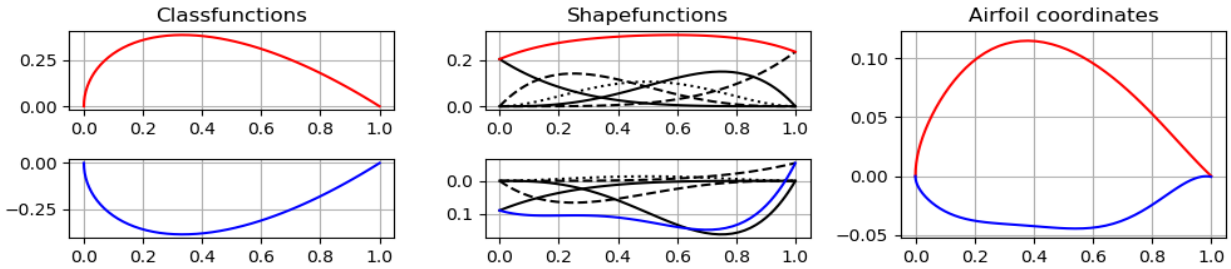

Figure 2. CST Parametrization of airfoil with fixed geometry

For airfoils with camber changing flaps, Boermans and van Garrel [10] proposed an airfoil design methodology with two distinct flap settings where either the top surface or the bottom surface is kink free. The resulting airfoil DU89-134-14, used on the ASH 26 and ASW 27 sailplanes marked the beginning of a new generation of flapped airfoils with long laminar flow regions on the bottom side up to 95%. In order to correctly parametrize this design methodology, a modification to the CST method is proposed here, shown in Figure 3. In addition to the parametrization of fixed geometry airfoils, a quadratic parabola is added to the top side coordinates. The parabola is scaled accordingly, so that the parabola crosses the trailing edge of the airfoil when the flap is deflected with the angle where the top side is kink free. Then the top side of the coordinates behind the flap axis are re-rotated so that the trailing edge ends at (1,0), shown as a dashed line in the right graph of Figure 3.

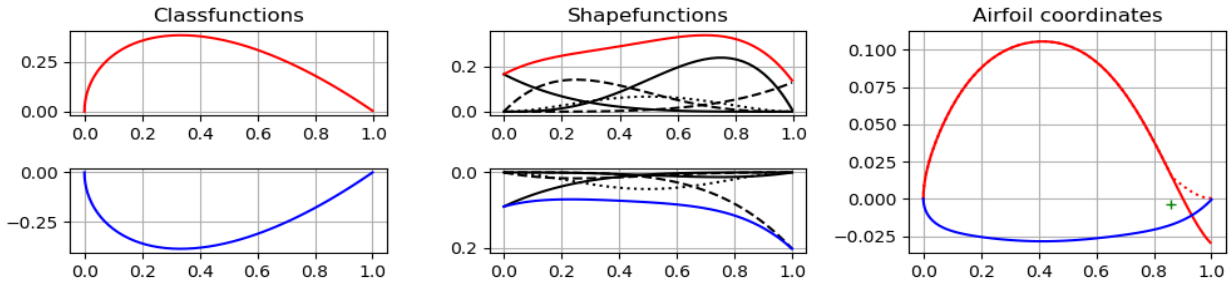

Figure 3. CST Parametrization of airfoil with camber changing flap

Optimization results of airfoils with fixed geometry and with camber changing flap

Figure 4 shows the calculated polars of the optimized airfoils as well as the polars of the reference airfoils. In the left two graphs the calculated (dashed) and the measured (solid) polars of the DU84-158 [11] airfoil are shown. Good agreement of measurements with calculations can be observed, although the lift in post stall is still overpredicted, but less than with default XFOIL 6.99. The preliminary design optimized airfoil (dotted) shows superior performance at high lift, but the lower corner of the laminar low drag bucket is at a higher c_l value. A redesign is recommended in order to obtain similar c_l values for the lower corner of the laminar low drag bucket. For the flapped optimized airfoil lower drag values were achieved compared to the DU89-134-14. Again, the laminar low drag bucket width of the

optimized airfoil is smaller than of the reference airfoil. The lift curve of the optimized airfoil shows a drop of lift coefficient beyond the laminar low drag bucket, which is detrimental for thermalling in turbulent conditions. Furthermore, a good airfoil performance can be reached by numerical optimization. This preliminary results suggest another optimization iteration by adaption of the design lift coefficients and postprocessing by inverse design.

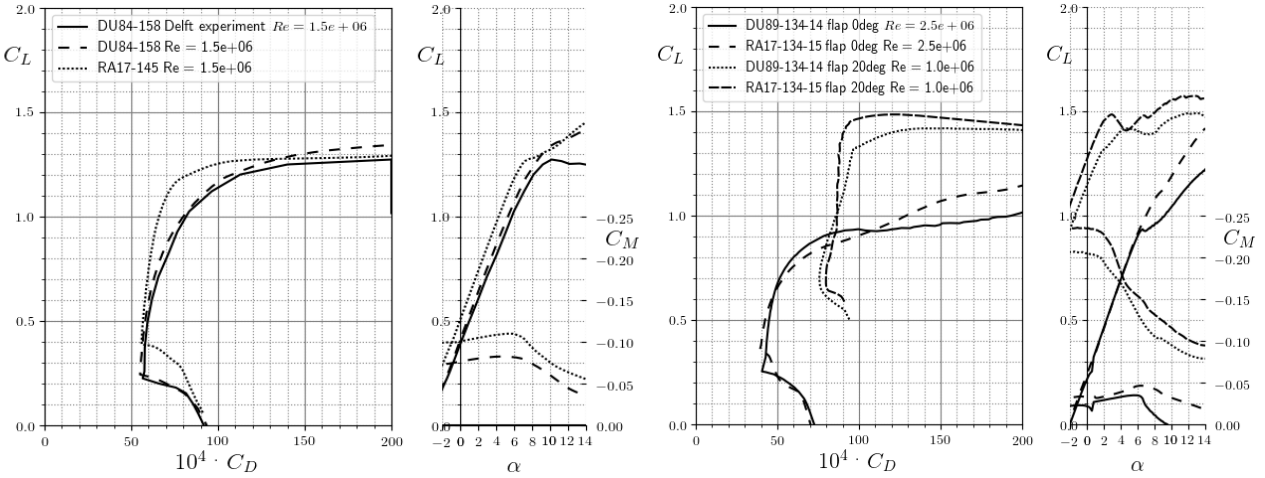

Figure 4. Polars of fixed geometry airfoils (left) and airfoils with camber changing flap (right)

CST parametrization of a variable leading edge geometry

A concept for a shape variable leading edge for sailplane design has been proposed by Weinzierl et al [12]. They also presented an aifoil reaching lift coefficients of $c_l = 1.8$. Thus enabling to increase the aspect ratio of the wing and the wing loading up to 70 kg/m^2, leading to a superior high speed performance. However, the presented airfoil suffered from separated turbulent flow on the flap top side, leading to high drag values and probably weak aileron effectiveness. The design of a morphing airfoil with conventional inverse and mixed-inverse methods seems to be complex because a geometrical match of unmorphed and morphed nose as well as the rigid center section is necessary. Therefore an extension of the CST method is presented which allows the parametrization of a variable leading edge geometry for numerical optimization. The upper and lower contour lines of the airfoil are decomposed into the camber line and the thickness distribution.

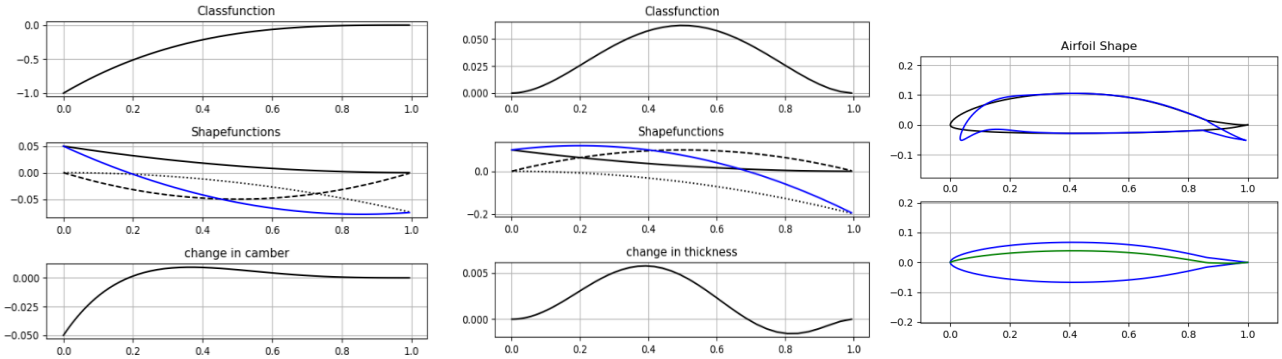

Figure 5. Class & shape functions for camberline(left), thickness distribution (middle), resulting airfoil (right)

Then, morphing is performed by adding additional functions to both curves. Compared to the undeformed airfoil parametrization, different class functions are used. For morphing of the thickness distribution, the class function from Eq. 2 is used, but with different exponents $N_1 = N_2 = 2.0$. The ψ coordinates are transformed to the area, where morphing is applied (Eq.4). ψ_e denominates the end of the morphing section. In this case, it was decided to morph the front 40% portion of the airfoil. Therefore, $\psi_e = 0.4$. In order to ensure a precise leading edge shape, which is important for a gentle stall behavior and good performance, the thickness of the leading edge part remains fixed. Consequently, the leading edge is supposed to undergo a rigid body motion only. At position ψ_s is the beginning of the section where the thickness distribution is changed. ψ_s is set equal to the leading edge radius.

$$\psi_t = \frac{\psi - \psi_s}{\psi_e - \psi_s} \quad and \quad \psi_c = \frac{\psi}{\psi_e} \tag{4}$$

The camber line morphing begins right at the leading edge, thus the coordinate transformation according to right part of Eq.4 is utilized. As class function, a parabola is utilized:

$$C_c = (\psi_c - 1)^{N_1} \quad with: \quad N_1 = 2.0 \tag{5}$$

A generic example of morphing an airfoil with the CST method is shown in Figure 5. The class functions are shown in the topmost figures. The resulting shape function is shown as a blue line in the centered figures, which is a sum of the weighted Bernstein polynomials (black lines). The resulting change in camber (left) or thickness (middle) is shown in the bottom diagram. The recomposed undeformed (black) and morphed airfoil (blue) is shown in the right image.

Optimization results of an airfoil with variable leading edge geometry

Figure 6 shows the airfoil shape of the optimized morphing wing airfoil. The airfoil is 11.6% thick, with a conventional camber changing flap of 16% length and 3.4% nose droop. In the bottom right picture the thickness distribution and the camber line in low lift configuration are shown. The minimum thickness curve is shown as the red dashed line. On the left half of the picture the calculated polars of the morphing airfoil compared to the DU89-134-14 with 0° and 20° flap deflection are shown. The morphing airfoil shows lower drag values in low lift configuration than the DU89-134-14. In high lift configuration similar drag values than the DU89-134-14 in 20° flap setting can be achieved, but at higher lift coefficients. It seems to be possible, that a lift coefficient of $c_l = 1.8$ can be reached with low drag values. This would enable to design a sailplane with a wing loading of 70 kg/m^2 with the same stall and thermalling speed of a conventional camber changing flap sailplane at wing loadings up to 60 kg/m^2, but with a large benefit for high speed performance. This demonstrates the performance potential of the variable leading edge geometry concept.

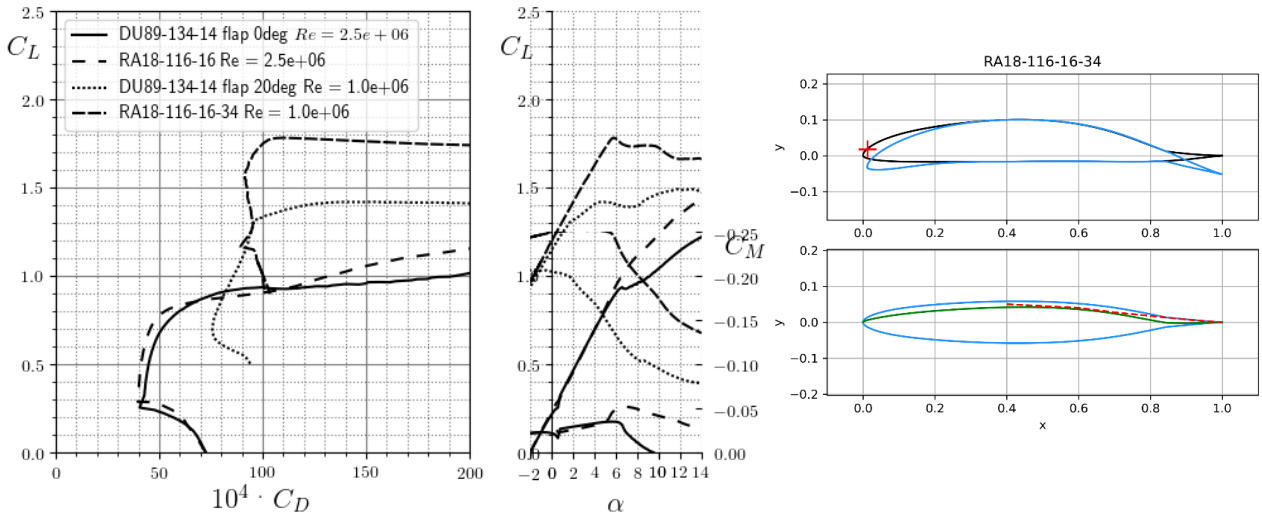

Figure 6. Calculated polars of DU89-134-14 and morphing airfoil (left), morphing airfoil shape (right)

References

[1]Kubrynski, K., 2012: Design of a Flapped Laminar Airfoil for High Performance Sailplane, 30th AIAA Appl. Aerodynamics Conf.

[2]Kulfan B.M., Bussoletti J.E. , 2006: “"Fundamental" Parametric Geometry Representations for Aircraft Component Shapes”, Int. 11th AIAA/ISSMO Multidisciplinary Analysis and Optimization Conference

[3]Drela, M., 1989: XFOIL: An Analysis and Design System for Low Reynolds Number Airfoils, Low Reynolds Number Aerodynamics. Lecture Notes in Engineering, Vol 54: 1-12.

[4]Rowan, T.H. 1990: Functional Stability Analysis of Numerical Algorithms, Dissertation, University of Texas, Austin.

[5]Nelder, J.A., Mead, R., 1965: A simplex method for function minimization. Computer Journal, Vol. 7: 308–313.

[6]Timmer, W.A., van Rooij, R.P.J.O.M, 2003: Summary of the Delft University Wind Turbine Dedicated Airfoils, Journal of Solar Energy Engineering, Vol 125 No 4: 488-496

[7]van Rooij, R.P.J.O.M., 1996: Modification of the boundary layer calculation in RFOIL for improved airfoil stall prediction. Report IW-96087R, Institute for Wind Energy, Delft University of Technology.

[8]Hansen, T.H., 2018: Airfoil optimization for wind turbine application, Wind Energy Journal, Online Version

[9]Ramanujam, G et al., 2016: Improving Airfoil Drag Prediction, Journal of Aircraft, Vol 53, No 6, pp 1844-1852

[10]Boermans, L.M.M., van Garrel, Design and Windtunnel Test Results of a Flapped Laminar Flow Airfoil for High-Performance Sailplane Applications ICAS-Paper 94-5.4.3

[11]Boermans, L.M.M., Waibel, G.: Aerodynamic and Structural Design of the Std. Class Sailplane ASW-24 ICAS-Paper 88-2.7.2

[12]Weinzierl, M., Achleitner, J., Baier, H., 2015: Highly Extensible Skin of a Variable Geometry Wing Leading Edge of a High-Performance Sailplane, Technical Soaring Vol 39 No 1: 4-9

Gefördert durch:

Bundesministerium für Wirtschaft und Energie

aufgrund eines Beschlusses des Deutschen Bundestages